



The Mars flyby of ROSETTA: an opportunity for infrared and microwave high-resolution sounding

Th. Encrenaz^{a,*}, A. Coradini^b, G. Beaudin^c, J. Crovisier^d, P. Drossart^a, S. Erard^e, B. Germain^c, S. Gulkis^f, Y. Langevin^e, E. Lellouch^a

^aDESPA, Observatoire de Paris, Meudon 92195, France

^bInstituto di Astrofisica Spaziale CNR, Via Fosso del Cavaliere, Roma 00133, Italy

^cDEMIRM, Observatoire de Paris, Paris 75014, France

^dARPEGES, Observatoire de Paris, Meudon 92195, France

^eInstitut d'Astrophysique Spatiale, Orsay 91405, France

^fJPL, Pasadena 91109, USA

Received 30 June 2000; received in revised form 7 February 2001; accepted 15 February 2001

Abstract

The Mars flyby of ROSETTA will provide a valuable opportunity for sounding, at high spatial resolution, the Mars atmosphere and surface in the infrared and microwave range. The VIRTIS infrared imaging spectrometer should be able to determine the surface mineralogy and temperature of the observed areas, the abundances of minor constituents (H₂O, CO), and possibly to study the atmospheric thermal profile. VIRTIS will complement the OMEGA and PFS infrared spectrometers on-board the Mars Express mission, expected to operate in Mars orbit at the time of the ROSETTA flyby. The MIRO microwave spectrometer is expected to provide information on the thermal profile, the H₂O vertical distribution, the temperature of the subsurface, and possibly the atmospheric winds. In addition, the Mars flyby of ROSETTA will provide the first opportunity for testing the VIRTIS and MIRO instruments, in particular for wavelength/frequency and photometry/radiometry calibration. © 2001 Elsevier Science Ltd. All rights reserved.

1. Introduction

There are still many unresolved questions regarding the composition of the Martian surface, as well as the seasonal and interannual evolution of its atmosphere. As an example, carbonates have been searched for on the Martian surface for decades, but, in spite of several tentative detections (Pollack et al., 1990; Clark et al., 1990; Lellouch et al., 2000), they have never been firmly identified so far. The search for carbonates and other mineralogic species on the Martian surface at high spatial resolution is still a major objective for future studies. Another important question deals with the present water cycle of Mars. A better knowledge of the water vapor vertical distribution is necessary to understand the mechanisms of water ice formation at the surface and in the clouds, and more generally, the sources and sinks of water as a function of the seasonal cycle.

Remote sensing spectroscopy in the infrared and millimeter range is an important tool for studying the chemical composition of the Martian atmosphere and surface. At short wavelengths, below about 4 μm, the spectrum is dominated by reflected or scattered sunlight, while thermal emission prevails at longer wavelengths. Infrared observations have been performed from the ground (see Soderblom, 1992, for a review), from the KAO (Pollack et al., 1990) and from space, either from Earth orbit (SWS on ISO; Lellouch et al., 2000) or from Mars orbit: IRS on Mariner 6 and 7 (Kirkland et al., 1998), IRIS on Mariner 9 (Hanel et al., 1972), ISM on Phobos (Bibring et al., 1991; Erard and Calvin, 1997), TES on MGS (Christensen et al., 1998). Information has been retrieved about the surface mineralogy, the composition of suspended dust and the column densities of minor constituents (H₂O and CO).

Ground-based millimeter heterodyne spectroscopy has been used since the 1970s (Kakar et al., 1977) to determine the thermal atmospheric profile from the analysis of CO transitions, observed with a resolving power as high as 10⁶ (Clancy et al., 1990; 1996; Lellouch et al., 1991a).

* Corresponding author. Tel.: +33-1-4507-7691; fax: +33-1-4507-2806.

E-mail address: therese.encrenaz@obspm.fr (Th. Encrenaz).

Table 1
 Characteristics of infrared and microwave instruments aboard ROSETTA and Mars express

	ROSETTA		Mars express	
	VIRTIS-M (IR)	VIRTIS-H	OMEGA (IR)	PFS (SW)
<i>Infrared spectrometers</i>				
Spectral band (μm)	0.93–5.03	1.95–5.00	0.9–5.3	1.2–5.0
Spectral resolving power	100–300	1200–3000	100–200	1000–4000
Spatial resolution (rad)	2.5×10^{-4}	5×10^{-4}	1.2×10^{-3}	2×10^{-2}
FOV with scan (deg)	3.6×3.6			
<i>Microwave radiometer/spectrometer</i>				
		MIRO (mm)		MIRO (submm)
Frequency (GHz)		189		547–579
Wavelength (mm)		1.58		0.54
Beamwidth (HPBW) (rad)		6×10^{-3}		2×10^{-3}
Spectral resolution				
Spectroscopic mode (kHz)				44
Continuum mode (MHz)		0.5		1.0
Observed transitions (GHz)				H ₂ ¹⁶ O (556.936) H ₂ ¹⁷ O (552.021) H ₂ ¹⁸ O (547.677) CO (5–4) (576.268)
Allocated spectral range per transition(MHz)				
With no freq.-switch				20 (all transitions)
With freq.-switch				30 (H ₂ ¹⁶ O) 20 (other transitions)

Since 1990, this technique has also been used to retrieve the vertical distribution of water vapor from transitions of HDO and H₂O (Encrenaz et al., 1991, 1995; Clancy et al., 1992, 1996). The high resolving power of heterodyne spectroscopy has also allowed the measurement of stratospheric winds from the Doppler shift of the CO transitions (Lellouch et al., 1991b; Théodore et al., 1993). The heterodyne technique, however, has never been used from space so far, apart from recent Earth-orbit submillimeter measurements by the SWAS satellite (Gurwell et al., 2000). The first opportunity to observe Mars at high spatial resolution will be provided by the flyby of Mars by the ROSETTA spacecraft in 2005.

The orbiter of the ROSETTA mission, designed for a long-term monitoring of a cometary nucleus (Wirtanen), is equipped with several remote-sensing instruments, including an infrared imaging spectrometer (VIRTIS) and, for the first time in a planetary mission, a microwave heterodyne receiver (MIRO). VIRTIS (Reininger et al., 1996; Coradini et al., 1998) consists of two channels, VIRTIS-M and VIRTIS-H. Both channels use gratings and HgCdTe detector

arrays, cooled at 70 K. VIRTIS-M is a mapping spectrometer which covers the 0.3–5.0 μm range with a spectral resolving power of about 100; VIRTIS-H is a high-resolution cross-dispersor spectrometer ($R = 2000$) operating between 2.5 and 5.0 μm (Drossart et al., 2000). The MIRO instrument (Gulkis et al., 2001) is a heterodyne receiver with two channels. It uses a 30-cm antenna and includes two receivers, one at 189 GHz (operating in the continuum mode) and the other around 557 GHz (operating in both continuum and spectroscopic modes). The submillimeter receiver (557 GHz) allows spectroscopy of H₂O and CO transitions with a resolving power as high as 10^7 . Technical characteristics of VIRTIS and MIRO are given in Table 1.

After its launch in January 2003, the ROSETTA spacecraft will first encounter Mars for the purpose of gravity assistance. This encounter thus provides the first opportunity for testing the ROSETTA instruments; in particular, wavelength/frequency calibration and flux calibration will be possible. In addition, the Mars observations will be of valuable scientific interest, as they will complement the monitoring of Mars by the Mars Express mission, planned to

Table 2
The Mars flyby of ROSETTA

Date	August 26, 2005
Day	948
V_{inf} (km/s)	7.26
V_{per} (km/s)	8.72
Minimum distance (km)	200
R_h (AU)	1.39
Δ (AU)	0.69
Sun–Earth–Mars angle ($^\circ$)	109
Sun–Mars–Earth angle ($^\circ$)	43

be in operation also at that time. VIRTIS-M and VIRTIS-H, respectively, show strong similarities with the OMEGA instrument and with the short-wavelength channel of the Planetary Fourier Spectrometer (PFS-SW) on-board Mars Express (see Table 1). Previous analyses, by ISM-Phobos in particular, have demonstrated the scientific capabilities of such instruments to sound the Martian atmosphere and surface (Rosenqvist et al., 1992; Erard and Calvin, 1997). In the case of MIRO, its performances have no equivalent on the Mars Express scientific payload, nor on any other past planetary missions. As demonstrated by Muhleman and Clancy (1995), in-orbit microwave observations are able to provide a unique scientific contribution on the Martian temperature field, the water vapor vertical distribution, and the atmospheric circulation. The Mars infrared spectrum is dominated by the signatures of CO_2 , CO and H_2O , also expected on comets. In the case of MIRO, the channels devoted to the observation of CO and of H_2O and its isotopes in comet Wirtanen will also be usable for the Mars observations. In general, the spectrometer will permit the observation of these transitions with a bandwidth of 20 MHz centered on the rest frequency of each transition, with a spectral resolution of 44 kHz. A special operation mode of the receiver, using a frequency-switching procedure, will permit us to use a bandwidth of 30 MHz centered on at least one spectral line (i.e. H_2^{16}O).

The Mars flyby of ROSETTA is expected to take place on August 26, 2005 (Table 2). At that time, the areocentric longitude L_s will be 282° (Kieffer et al., 1992); the mean surface pressure, averaged over the disk, will be close to its maximum (7.5 mbar; Kieffer et al., 1992; Zurek et al., 1992). The expected column density of H_2O near the equator will be in the range 1–10 pr- μm (or 0.1–1.2 cm-am; Jakosky and Haberle, 1992). CO_2 is the main atmospheric constituent (95% per volume). The CO mixing ratio is 7×10^{-4} (Kieffer et al., 1992).

2. The Mars flyby

The geometrical configuration is shown in Fig. 1. Due to the Earth position (Sun–Mars–Earth angle = 43°), an occultation of the spacecraft by Mars (as seen from Earth) occurs between -39 and -2 min with respect to the closest

approach. In order to reduce complexity as much as possible, we have assumed that no motion of the platform would take place during the flyby. As a result, the spacecraft will observe the planet with a constant pointing angle, from one limb to another, and nadir will be observed only once. The pointing angle will be fixed along the sequence, but its choice will be optimized for a maximum scientific return.

In order to favor day-time observations (more interesting for VIRTIS and several other instruments) we have selected two possible pointing angles (antisun–spacecraft–line of sight), -30° and 8° (Fig. 1(a) and (b)). Both directions are compatible with the positioning constraint of the VIRTIS radiator. Any intermediate direction would be also acceptable. The observation parameters associated to these two configurations are given in Tables 3a and 3b. Observations take place at $[-4 \text{ min}, +12 \text{ min}]$ in the first case, and at $[-1 \text{ min}, +27 \text{ min}]$ in the second case. In the latter case, due to the relative Doppler shift of the spacecraft versus the line of sight and the limited available bandwidth (20 MHz for each transition), the central frequency of the 557 GHz channel of MIRO needs to be shifted by use of the frequency-switching procedure. The first case is more favorable for acquiring a high spatial resolution; we also note that, in this case, the first observations occur on the dark side, and that the observation sequence has to start within the occultation phase. The second case provides a longer observation time, but with a reduced spatial resolution; the 557 GHz H_2^{16}O line center can be observed during the whole sequence but the centers of the other transitions are outside the available bandwidth. Thus, the second case is not favorable for microwave observations.

A third case could be considered, with the line of sight aligned with nadir at pericenter. This geometry corresponds to a pointing angle of -58° . This configuration provides a minimum Doppler shift with respect to the line of sight (between -2.4 and $+2.4$ MHz) and is thus optimized for MIRO observations. It would also provide a maximum spatial resolution on the Mars surface. However, a significant part of the observing sequence would take place on the night side. Also, the high phase angle may not be compatible with the spacecraft positioning constraints. In view of these comments, the first case (pointing angle of -30°) appears as a good compromise for infrared and microwave observations.

3. VIRTIS observations

3.1. VIRTIS-M

3.1.1. The VIRTIS-M spectrum

Fig. 2, calculated for a simulation of the Mars spectrum, as seen by the OMEGA experiment, on the basis of a model developed by Erard (1998), provides a good approximation of the Mars spectrum as will be seen with VIRTIS-M. It shows spectra corresponding to various terrains (warm

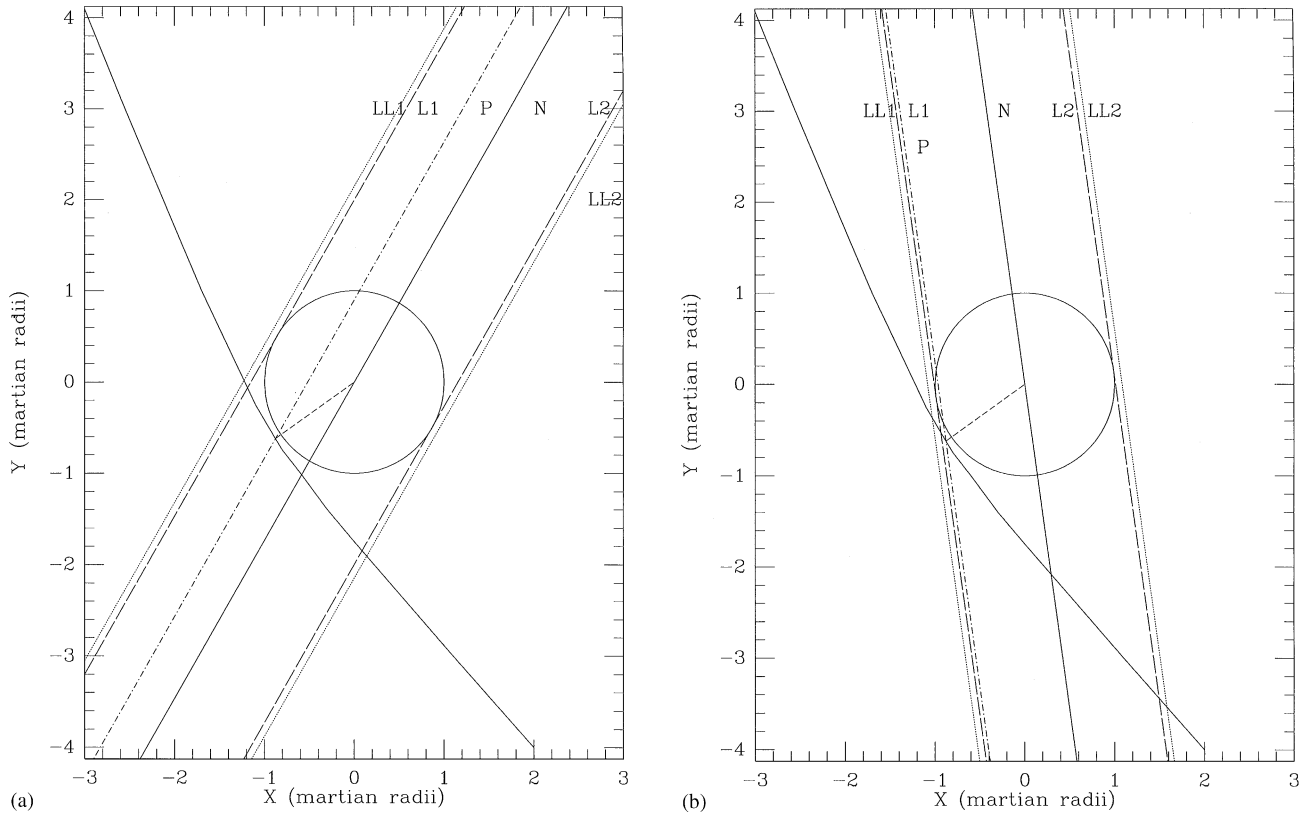


Fig. 1. Geometry of encounter. (a) Fixed pointing angle: -30° (Case 1); (b) fixed pointing angle: 8° (Case 2). The Sun direction is along the $-Y$ axis. The Sun–Mars–Earth angle is 43° . The spacecraft moves from the top ($X < 0, Y > 0$) to the bottom ($X > 0, Y < 0$) along its trajectory. Fixed-pointing angle: antisun–spacecraft–line of sight; LL1: line of sight at $z = 250$ km above the first limb; L1: first limb; P: pericenter; N: nadir; L2: second limb; LL2: line of sight at $z = 250$ km above the second limb. The time sequences for both cases 1 and 2 are indicated in Tables 3a and 3b.

Table 3
Observing sequence^a

Event	T (min)	D_M (km)	VIRTIS-H pixel (km)	MIRO pixel (km)	V (km/s)	V_D (km/s)	Δv (MHz)
(a) Case 1 (fixed pointing angle: -30°)							
LL1	-4.2	2000	1.0	4.0	8.6	4.8	-9.0
L1	-3.8	2160	1.1	4.4	8.6	4.8	-9.0
P	0	270	0.1	0.5	8.7	4.2	-7.8
N	+3.6	600	0.3	1.2	8.6	3.4	-6.3
L2	+11.0	5200	2.6	10.4	8.2	2.6	-4.8
LL2	+11.5	5330	2.7	10.7	8.1	2.6	-4.8
(b) Case 2 (fixed pointing angle: 8°)							
LL1	-1.3	730	0.4	1.4	8.7	8.0	-14.9
L1	-0.2	1270	0.6	2.5	8.7	8.0	-14.9
P	0.0	730	0.4	1.4	8.7	8.0	-14.9
N	13.2	3800	1.9	7.6	8.0	6.7	-12.5
L2	26.1	12270	6.1	24.5	7.7	6.4	-11.9
LL2	27.3	12670	6.3	25.3	7.6	6.4	-11.9

^aNote: (1) Fixed pointing angle: Antisun–spacecraft–line of sight. (2) LL1: line of sight at $z = 250$ km above the first limb. (3) L1: first limb. (4) P: pericenter. (5) N: nadir. (6) L2: second limb. (7) LL2: line of sight at $z = 250$ km above the second limb. (8) T : time with respect to closest approach. (9) D_M : distance to the Mars disk. (10) V : velocity of the spacecraft with respect to Mars. (11) V_D : velocity of the spacecraft along the line of sight. (12) Δv : Doppler shift of the 557 GHz $H_2^{16}O$ transition.

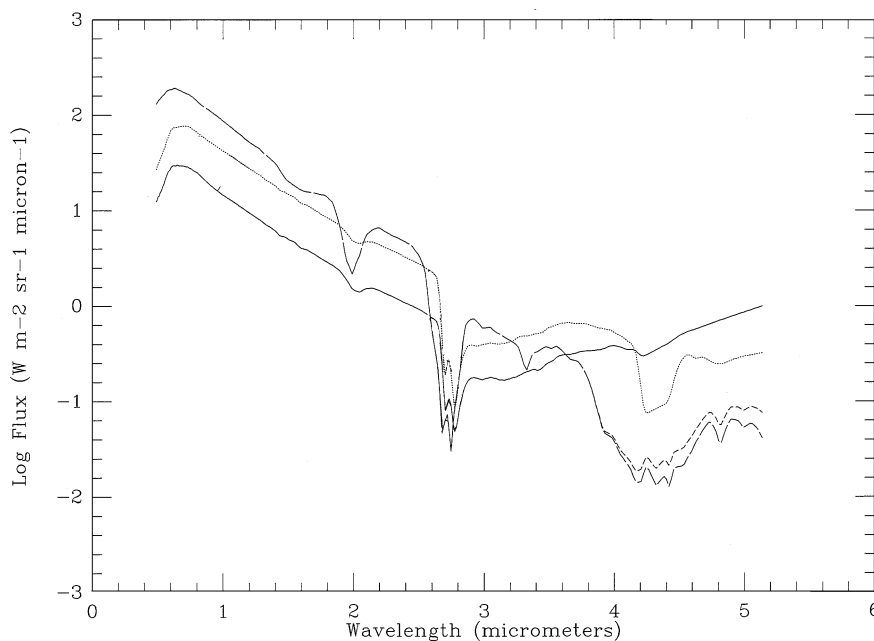


Fig. 2. The spectrum of Mars between 0.4 and 5.2 μm , as derived by a model developed by Erard (1998). Solid line: dark area; dotted line: bright area; short-dashed: warm polar cap; long-dashed: cold polar cap.

and cold ice caps, corresponding to different brightness temperatures measured by IRTM; dark and bright areas), seen with a phase angle of 20° and an emission angle of 10° . The spectral resolving power is about 100, i.e. comparable to or slightly lower than the expected resolving power of VIRTIS-M. CO_2 gaseous signatures appear at 2.0, 2.7, 4.25, 4.85 and 5.2 μm ; the CO (1–0) band is visible at 4.7 μm (the (2–0) band at 2.35 μm is too weak to be detected on this scale). The broad absorption between 3.0 and 3.5 μm is due to hydrated silicates; in the polar cap spectra, the broad absorption at 4–5 μm is due to CO_2 ice.

3.1.2. Expected S/N ratio and integration time

Calculations by Reininger et al. (1996) show that an S/N of at least 100 is expected over the whole IR range, for a planetary surface located at 3.2 AU with an albedo of 0.04 and a temperature of 167 K, and with an integration time of 3 s. For estimating the S/N ratio on Mars, we assume a mean albedo of 0.2 and a mean surface temperature of 210 K (these quantities however are expected to exhibit strong variations over the Martian surface during the flyby). We also assume, on the basis of previous analyses (Lellouch et al., 2000), that the Martian spectrum is dominated by reflected sunlight for $\lambda < 4 \mu\text{m}$ and by thermal emission for $\lambda > 4 \mu\text{m}$. Under these assumptions, we derive an S/N as high as 250 in 1 s of integration time at the surface of Mars, over the whole 1–5 μm spectral range.

The size of the VIRTIS-M map is a 3.6° square. In the absence of spacecraft motion, in the first case (pointing angle of -30°), the most resolved map (at pericenter) would be

about $35 \times 35 \text{ km}$ (pixel resolution: 80 m for $\lambda > 1 \mu\text{m}$), with an emission angle of about 30° ; in the second case (pointing angle of 8°), the most resolved map would be about $50 \times 50 \text{ km}$, one minute after perigee, with an emission angle of about 60° . However, as the shortest acquisition time is about 0.3 s, the spacecraft motion (8.7 km/s at closest approach) considerably degrades (up to a few km) the spatial resolution along this axis.

3.2. VIRTIS-H

3.2.1. The VIRTIS-H spectrum

The infrared spectrum of Mars has been observed between 2.3 and 45 μm by the short-wavelength spectrometer (SWS) of the ISO mission, with a spectral resolution comparable to the one of VIRTIS-H (de Graauw et al., 1997; Lellouch et al., 2000). Fig. 3 shows a composite spectrum of Mars in the 2.0–5.0 μm range, including the ISO-SWS data for $\lambda > 2.36 \mu\text{m}$ and a synthetic spectrum, calculated under the ISO conditions, for $\lambda < 2.36 \mu\text{m}$. Spectroscopic data were taken from the GEISA data bank (Jacquinot-Husson et al., 1999) and the reflected sunlight component, integrated over the disk, was determined from a line-by-line calculation using a Voigt profile for the line shapes. The ISO data refer to the entire disk, which was 6.4 arcsec in diameter. At the time of the ISO-SWS observations shown here (July 31, 1997; $L_s = 157^\circ$), the mean surface pressure was 5 mbar, and the H_2O column density was about 15 pr- μm (Burgdorf et al., 2000; Lellouch et al., 2000). The standard value of 7×10^{-4} was used for the CO mixing ratio (Lellouch et al.,

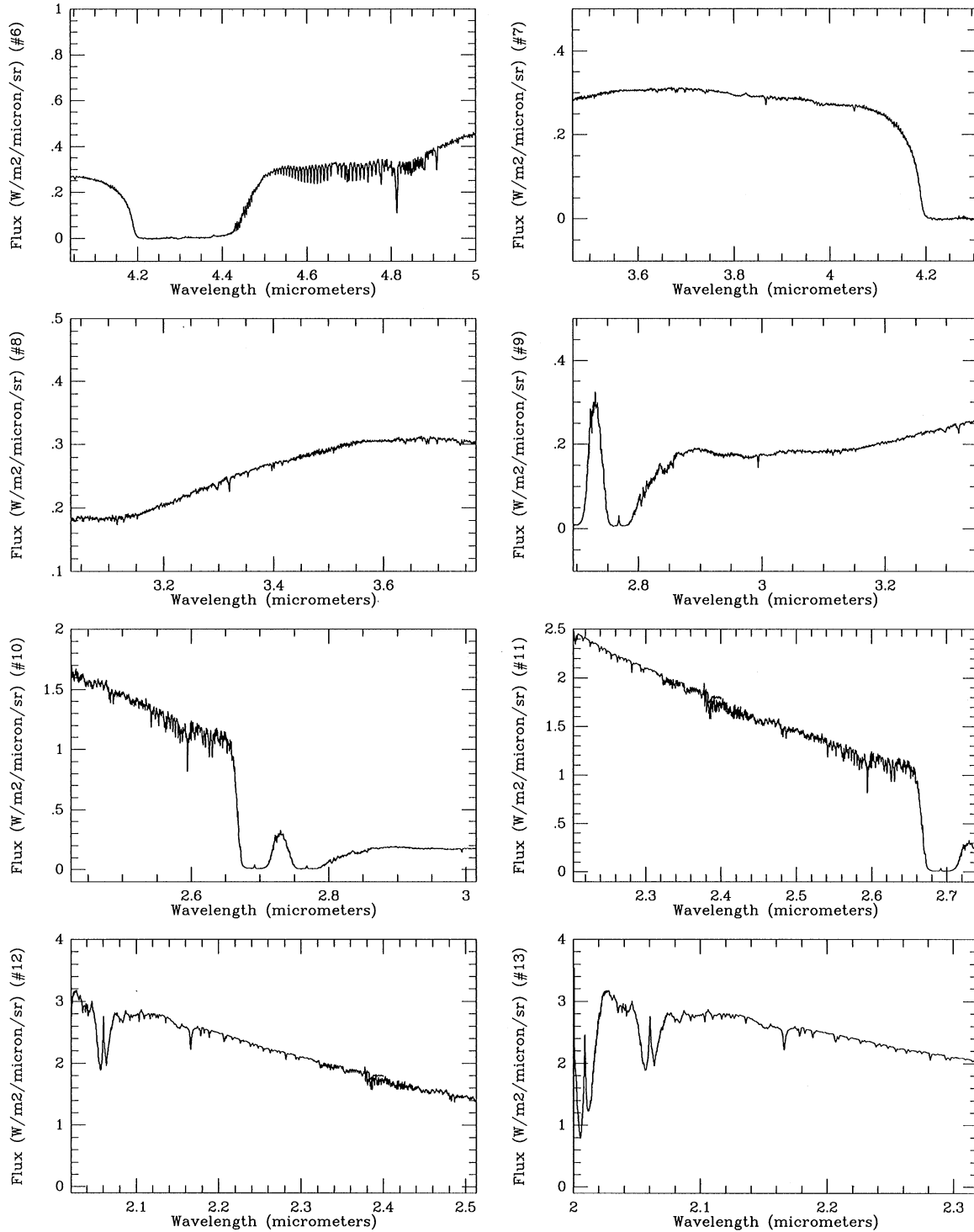


Fig. 3. A composite spectrum of Mars as will be observed by the 8 grating orders of VIRTIS-H. From left to right and top to bottom: Grating orders nos. 6 to 13 (see Table 5). For wavelengths higher than 2.4 μm , ISO data are used. Below this wavelength, a synthetic spectrum, corresponding to the same atmospheric parameters, is shown. Note that the 3.0–3.5 μm part of the spectrum may strongly vary as a function of location on the Mars surface, as shown in Fig. 2.

2000). The solar spectrum was taken from the HITRAN solar database (Kurucz, 1995). In Fig. 3, the spectrum is displayed according to the 8 orders of VIRTIS-H, from Order nos. 6 to 13.

3.2.2. Expected S/N ratio and integration time

Table 4 shows the expected S/N for 1 s integration time, calculated on the basis of the VIRTIS S/N nominal curve (updated from Reininger et al., 1996), which corresponds

Table 4
Estimate of S/N for VIRTIS-H (1 s integration time)^a

λ (μm)	Φ_M ($\text{W}/\text{m}^2/\mu\text{m}/\text{sr}$)	R	S/N (1)	S/N (2)
2.0	2.0	0.6	180	570
2.5	1.5	1.0	200	1060
3.0	0.2	0.3	200	320
3.5	0.3	0.8	160	680
4.0	0.3	1.0	140	370
4.5	0.3	—	130	130
5.0	0.4	—	20	20

^aNote: (1) Φ_M : Flux of Mars. (2) R : Reflectivity of the Mars spectrum (solar component). (3) S/N (1): Estimated S/N for $a = 0.2$, $R_h = 3.2$ AU, $T_s = 217$ K (updated from Reininger et al., 1996). (4) S/N (2): Estimated S/N for Mars spectrum ($a = 0.2$, $R_h = 1.39$ AU, $T_s = 217$ K), taking into account the Martian reflectivity. (5) NB: Reflected component is assumed for $\lambda < 4 \mu\text{m}$ and thermal emission for $\lambda > 4 \mu\text{m}$. At $4 \mu\text{m}$, an equal contribution of both components is assumed.

to a planetary surface at a heliocentric distance of 3.2 AU, with an albedo of 0.2 and a temperature of 217 K. The albedo and temperature values are adequate for mean Martian conditions; they strongly vary locally, however, over the Martian disk, and the shape of the Martian infrared spectrum changes accordingly (Fig. 2). As a mean value, we assumed the shape of the Martian spectrum as observed by ISO (Fig. 3). We estimated the S/N ratio of the Mars VIRTIS-H spectrum by assuming, as in the case of VIRTIS-M, reflected solar radiation below $4 \mu\text{m}$ and thermal emission above. It can be seen that the S/N shows a very large dynamical range between 2.0 and $5.0 \mu\text{m}$. An integrating time of 1 s is required in order to obtain an S/N of 20 at $5 \mu\text{m}$.

In the absence of spacecraft motion, the best spatial resolution for VIRTIS-H observations would be about 0.3 km in the first case and 1.2 km in the second case. These values correspond to a co-addition of three individual pixels (see Tables 3a and 3b). However, due to the spacecraft motion, the projected displacement over the Martian surface is several km in 1 s. The shortest acquisition time for VIRTIS-H is 0.3 s. Even in this case, the spatial resolution will thus be degraded up to a few kilometers in the direction parallel to the spacecraft motion.

3.3. VIRTIS calibration

3.3.1. Wavelength calibration

Internal calibration is used for photometric and spectral purposes. The photometric calibration uses, for each channel, a tungsten lamp through the calibration shutter placed at the entrance slit of each spectrometer.

External wavelength calibration will be provided by comparison with known spectral signatures of the Martian atmosphere. Table 5 shows the list of the lines which can be used as wavelength calibrators in the different grating orders of VIRTIS-H. We note that the CO_2 and CO calibrators are expected to show slightly stronger absorptions (as the mean surface pressure is expected to be higher than in

Table 5
Wavelength calibrators for VIRTIS-H

Order no.	Wavelength range	Calib. wavelength	Species
6	4.041–5.000	4.0524	Solar line
		4.8146	CO_2
		4.5–4.8 4.9080	CO (1–0) H_2O
7	3.464–4.307	3.8667, 4.0524	Solar lines
		3.3201	Solar line
8	3.031–3.769	3.3201	Solar line
		3.0033	H_2O
9	2.694–3.350	2.5419, 2.6258	Solar lines
		2.5944, 25946 ^a	H_2O
		2.5960	H_2O
10	2.204–2.741	2.5419, 2.6258	Solar lines
		2.5944, 25946 ^a	H_2O
11	2.021–2.513	2.1661	Solar line
		2.32–2.38	CO (2–0) at high airmass
12	2.000–2.319	2.1661	Solar line
13			

^aUnresolved at VIRTIS-H resolution.

the ISO case), while the H_2O lines should be weaker. In all cases, observations close to the limb will show enhanced absorption features of all atmospheric features, while the solar lines will stay constant. The ISO data, which were taken on the entire disk, correspond to a mean airmass of about 1.6 (emission angle: 50°).

3.3.2. Photometric calibration

In the case of the photometric calibration, due to the variety of terrains which will be scanned by the instruments, it will not be possible to check the internal photometric calibration of VIRTIS, on the basis of these data only. The absolute calibration is expected to be tested from a comparison with data taken at the same place by OMEGA and PFS/Mars Express, and from a modeling of the photometric functions.

3.4. Scientific interest of VIRTIS observations

As mentioned above, the VIRTIS instrument shows strong similarities with the two infrared spectrometers which will be flown on the Mars Express mission, OMEGA and PFS-SW (Table 1). OMEGA has the same spectral range as VIRTIS-M and comparable spatial and spectral resolving powers. The short-wavelength channel of PFS covers the spectral range of VIRTIS-H with comparable spatial and spectral resolutions. The advantage of VIRTIS, however, lies in the much higher sensitivity of its detectors.

3.4.1. VIRTIS-M

The Martian surface observed by VIRTIS during the Mars flyby of ROSETTA is expected to exhibit strong mineralogic variations. Bright areas are believed to be regions of heavy dust accumulation (Amazonis, Arabia) or limited dust accumulation (Chryse, Elyseum). Dark regions, as observed in Acidalia and Syrtis Major, are interpreted as exposed rocks from which the dust layer has been removed, or may also,

in some cases, be due to the accumulation of dark sands. These various terrains will exhibit very different spectral signatures between 1 and 5 μm (Erard and Calvin, 1997), and their mineralogy will be characterized by infrared imaging spectrometers like VIRTIS-M and OMEGA.

VIRTIS-M will provide a mapping of a narrow track (about 30–50 km wide near closest approach) at low latitudes, from limb to limb. Information will be retrieved upon the solid signatures along this band (in particular in the band of the hydrated silicates, which is highly variable as shown in Fig. 2), and upon the surface temperature. Intermediate albedo regions with high thermal inertia (e.g. Oxia Palus) are interpreted as regions of duricrust formation. In this case, VIRTIS-M, together with OMEGA and TES, may help determine the cement agent (sulfates, oxides, etc.). In dark areas, high signal-to-noise spectra will help characterizing the volcanic materials. These data should provide a useful complement to TES and OMEGA data.

3.4.2. VIRTIS-H

In addition to mineralogic information, VIRTIS-H will provide a determination of several atmospheric parameters, namely the H_2O and CO abundances, and possibly upon the thermal profile from limb to limb. The method, described in more detail below, is the following: in the reflected sunlight component, information can be retrieved on the surface pressure (from CO_2 at 2.0 μm) and on the H_2O and CO column densities independently of the thermal profile. Once these parameters are determined, the thermal part of the VIRTIS spectrum can be used to retrieve information upon the thermal profile in the troposphere.

Information about the local surface pressure will be obtained from the depths of individual lines of the ($2\nu_1 + \nu_3$) CO_2 band near 2 μm . Such a method was used by ISM-Phobos for the purpose of altimetry studies (Bibring et al., 1991) assuming a constant pressure over the Martian disk at a given altitude. Since the Martian topography is now accurately known from the MOLA radar measurements of Mars Global Surveyor, the CO_2 measurement can now be used for monitoring the local surface pressure. At 2 μm , the expected S/N in 1 s is about 560 (Table 4). The depth of the CO_2 band is in the range of 50% or more (Fig. 3). By comparison with the previous analysis performed with the ISM data, we estimate that pressure fluctuations could be retrieved with a precision of about a few percent.

In the case of H_2O , the most suitable spectral range is around 2.6 μm . Fig. 4 shows a calculation of several H_2O transitions of the ν_3 band, corresponding to nominal conditions at the time of the Mars flyby (H_2O mixing ratio of 3×10^{-5} at the surface, column density of 2.5 pr- μm). We note that no saturation is expected under these conditions. Calculations were performed for two emission angles, 0° (nadir) and 85° . The depth of the strongest H_2O line, at 2.595 μm , is about 10% in the first case and 30% in the sec-

ond case. Calculations show that, with an expected S/N of about 1000 in 1 s (Table 4), assuming the nominal abundance of 2.5 pr- μm for the H_2O column density, this quantity could be retrieved from limb to limb with an accuracy of about a few percent.

In the same way, the CO abundance will be mapped with high accuracy using the CO (2–1) band at 2.3 μm (Fig. 5). Due to the long lifetime of carbon monoxide, the CO mixing ratio is expected to be constant with height. However, previous infrared observations with ISM-Phobos seemed to indicate significant variations of the CO abundance in localized areas of the Martian disk (Rosenqvist et al., 1992). The ISM data, however, had a low spectral resolution ($R = 60$). The VIRTIS-H observations, at much higher spectral resolution ($R = 2000$), will be able to reiterate the measurement of CO from limb to limb and to search for possible local variations with a precision of a few percent; we note, however, that an inhomogeneous distribution of atmospheric dust could possibly affect the precision of the measurements. The high spectral resolving power of VIRTIS-H (with regard to OMEGA) and its high sensitivity (with regard to PFS) will be useful, in particular, to disentangle the atmospheric and mineralogic contributions in the 2.3 μm range (Clark et al., 1990; Encrenaz and Lellouch, 1990).

Once the CO abundance and the surface pressure are determined, information about the thermal profile in the lower troposphere could be retrieved, at least in the dark areas, from the thermal bands of CO_2 (ν_3 band at 4.25 μm) and CO (1–0 band around 4.7 μm).

The high sensitivity of VIRTIS-H will also be needed for accurately measuring the low fluxes previously detected by ISO-SWS in the center of the strong CO_2 bands (Lellouch et al., 2000). In the reflected sunlight component, in the center of the 2.7 μm band, information will be retrieved upon the dust optical depth and possibly its vertical distribution (Titov et al., 2000). At 4.25 μm , a weak fluorescence emission is detectable (Lellouch et al., 2000). These data will provide information upon the atmospheric temperature structure in the mesosphere.

The information derived from VIRTIS will be directly comparable to the data taken by OMEGA and PFS. In view of their improved spectral resolution and detector sensitivity, the VIRTIS data should be able to provide a significant complementary dataset.

4. MIRO observations

MIRO is a dual-frequency heterodyne receiver, equipped with a continuum channel at 188.2 GHz and a spectroscopic channel in the 547–577 GHz range, pretuned to observe a number of cometary molecular transitions. Among the lines of interest for Mars are H_2O and its isotopes (H_2 ^{16}O at 556.936 GHz, H_2 ^{17}O around 552.021 (hyperfine structure), H_2 ^{18}O at 547.677 GHz), and CO at 576.710 GHz. The line expected to be of most interest is the H_2 ^{16}O transition.

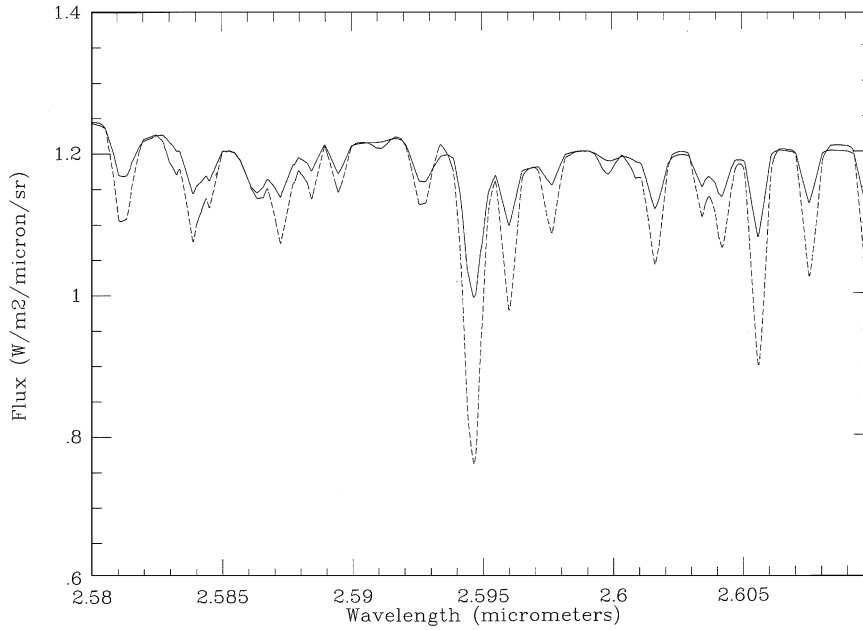


Fig. 4. Variation of the depths of the H₂O lines in the 2.58–2.61 μm range as a function of the emission angle. Solid line: nadir observations (emission angle = 0°); dashed line: emission angle = 85°. The H₂O column density is 2.5 pr-μm, typical of the expected conditions at the time of the Mars flyby.

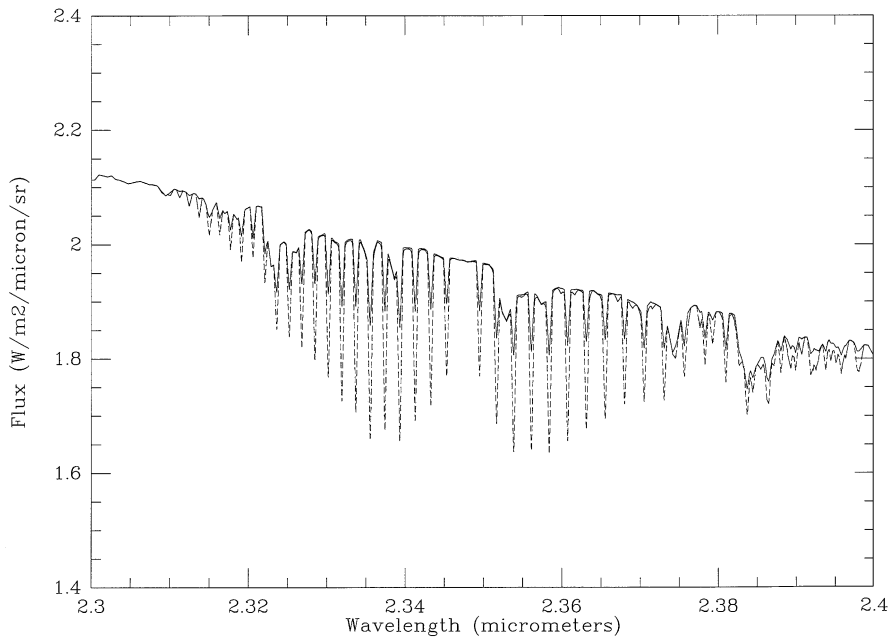


Fig. 5. The CO (2–1) band observed between 2.3 and 2.4 μm for emission angles of 0° (nadir; solid line) and 85° (dashed line).

MIRO has been optimized for the simultaneous observation of several cometary lines at high spectral resolution within the band of a single spectrometer. Therefore, the receiver operates at a pre-tuned frequency and each line is observed within a limited (20 MHz) spectral band. This is adequate for the observation of cometary lines, which are narrow (about 1 km/s), but this is not an optimum configuration for the Martian atmospheric lines which are

much broader, and affected by a significant Doppler shift during the flyby. Thus, an important limitation comes from the restricted bandwidth, limited to 20 MHz around each central frequency in the absence of frequency-switch. As mentioned above, the nominal configuration (case 1, pointing angle of -30° ; Table 3a) allows the observation of all line centers, and is thus favored for this reason.

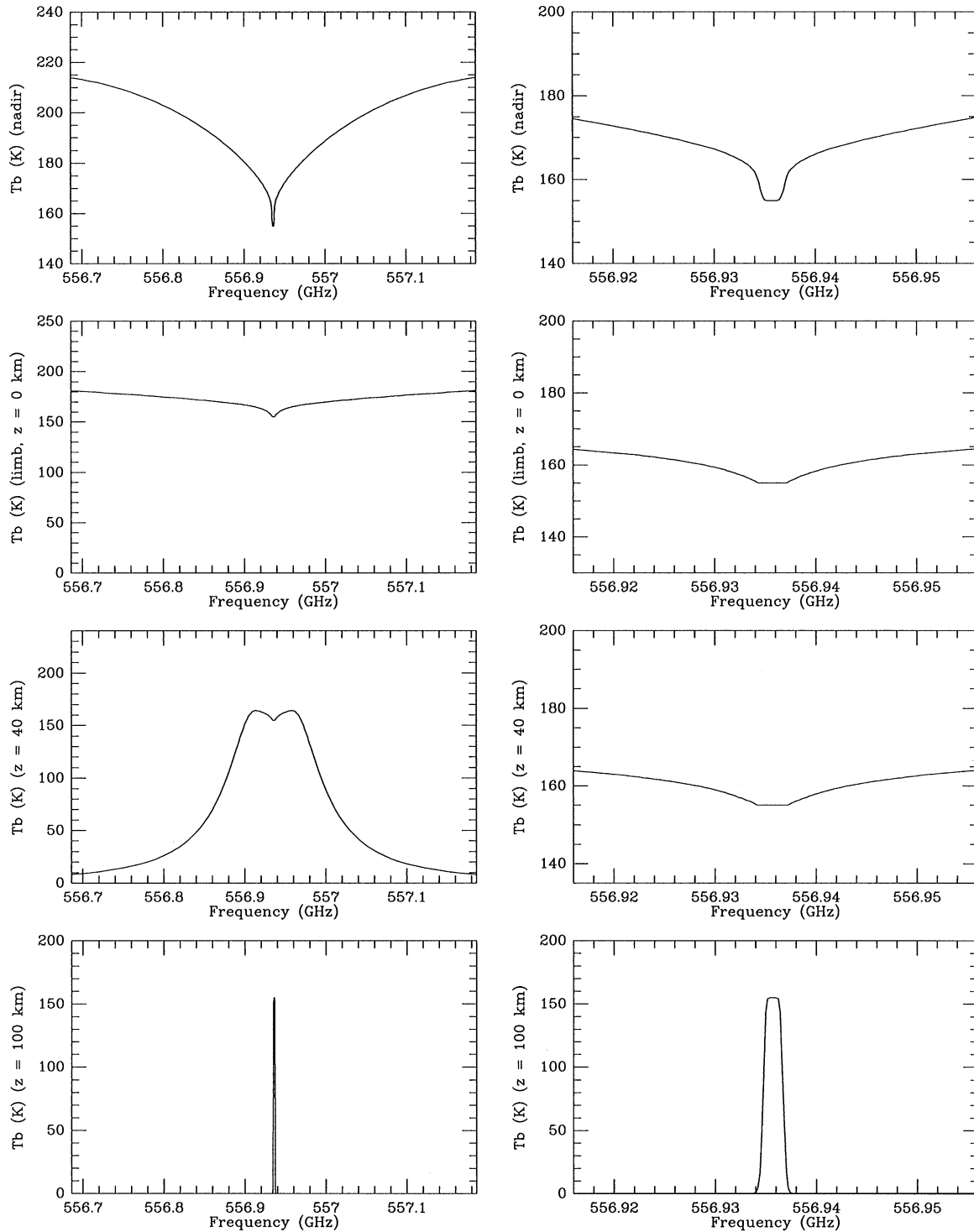


Fig. 6. The H_2^{16}O transition at 556.936 GHz, calculated for nadir, limb and off-limb observations. Left side: 0.5 GHz bandwidth; right side: 40 MHz bandwidth. The water column density is 2.5 pr- μm (expected conditions of flyby observations). z is the altitude above the limb, in km.

4.1. Spectral lines observed with MIRO

Figs. 6–9 show the expected profiles of H_2^{16}O , H_2^{17}O , H_2^{18}O and $\text{CO}(5-4)$, for nadir orientation, limb orientation, and off-limb observations (at altitudes of 40 and 100 km

above the limb). Each profile was computed for a single line of sight, i.e. at infinite spatial resolution, in order to illustrate the evolution of the line profile. H_2O calculations were performed with a H_2O mixing ratio of 3×10^{-5} , corresponding to a column density of 2.5 pr- μm , typical of

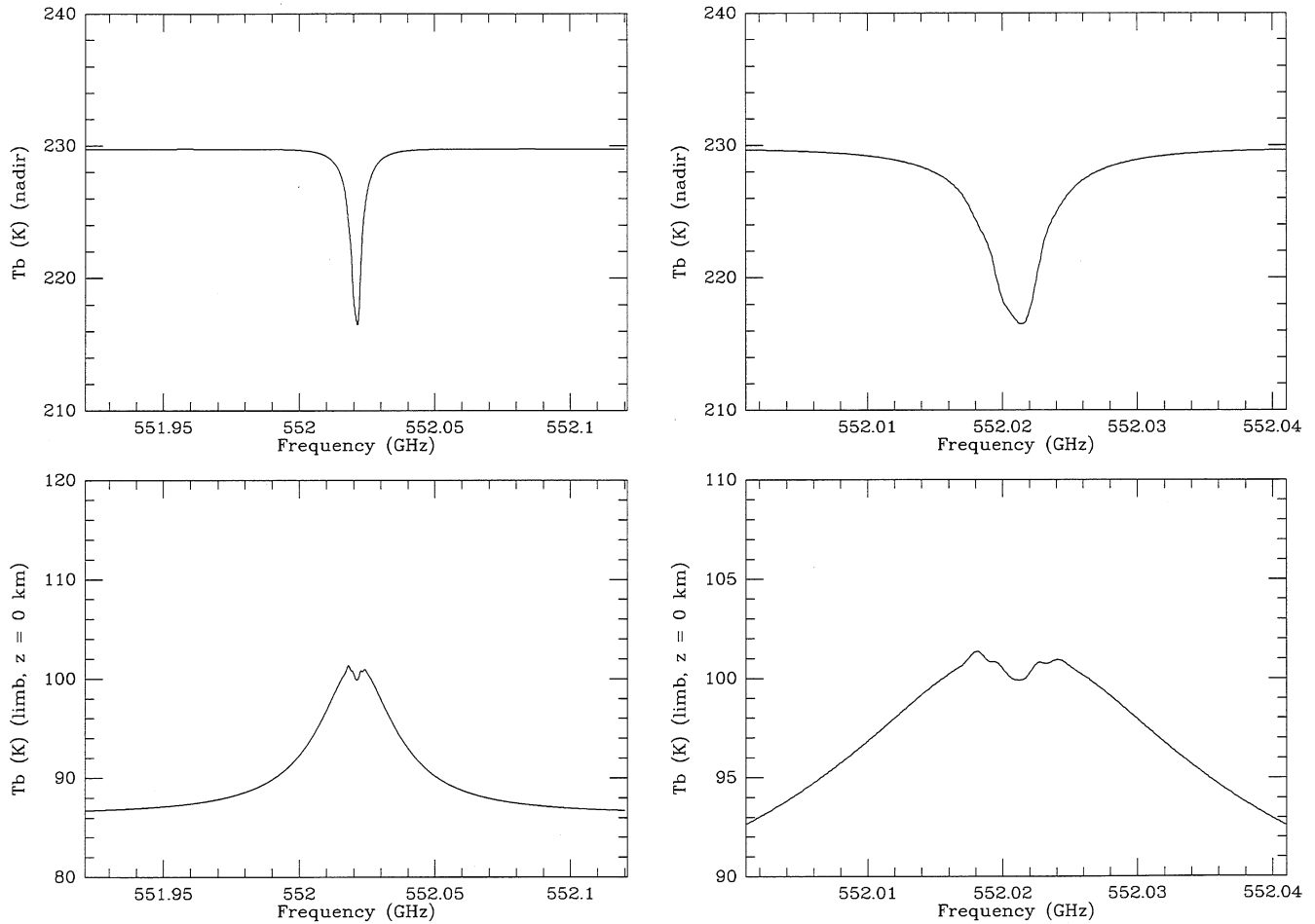


Fig. 7. The H_2^{17}O transition around 552.021 GHz, calculated for nadir and limb observations. Left side: 0.2 GHz bandwidth; right side: 40 MHz bandwidth. Due to hyperfine structure, the transition is splitted into seven multiplets.

the expected Martian conditions at the time of flyby. In all figures, the left side shows the full line profiles between ± 250 MHz (± 100 MHz for H_2^{17}O), and the right side shows the part which will be actually seen by MIRO. As the Doppler shifts of these lines will evolve during the flyby (depending upon the observing conditions), the right-side profiles have been plotted in a bandwidth of ± 20 MHz.

It can be seen that the line profiles vary very much as a function of the observed position on the planet. The H_2^{18}O and CO transitions are very strong, so that only the central core will be observed at nadir and limb position. The lines should be still observable at off-limb positions, up to a height above 100 km. The H_2^{17}O transition is weak enough to be fully observable in the available bandwidth on all surface observations; the H_2^{18}O line presents an intermediate case.

4.2. Expected S/N and integration time

The expected sensitivity of the submillimeter receiver, in the spectroscopic mode, is 2 K for a spectral resolution of

300 kHz and an integrating time of 2 min (Gulkis et al., 2001). This corresponds to an S/N between 75 and 100 for all surface observations, in the case of all transitions; for off-limb observations of H_2^{16}O , the expected S/N is about 75 at the center. However, due to the high velocity of the flyby phase, a 2-min interval corresponds to a motion of several hundreds of km over the Martian surface. It is thus necessary to reduce the integration time as much as possible. The shortest integration time for MIRO spectroscopic observations is 5 s, which corresponds to a projected spatial resolution of about 20 km. With such an integration time, the S/N will be reduced to 15–20 for all surface observations, and to about 15 for off-limb observations of H_2^{16}O .

In the continuum mode, the expected sensitivity, for 1 s integration time, is 0.08 K at 188 GHz and 0.16 K at 557 GHz. The brightness temperature of Mars will thus be measured with an S/N of about 2600 at 230 GHz and 1300 at 557 GHz, in 1 s integration time. In the observing sequence, the continuum and spectroscopic measurements will be carried out simultaneously.

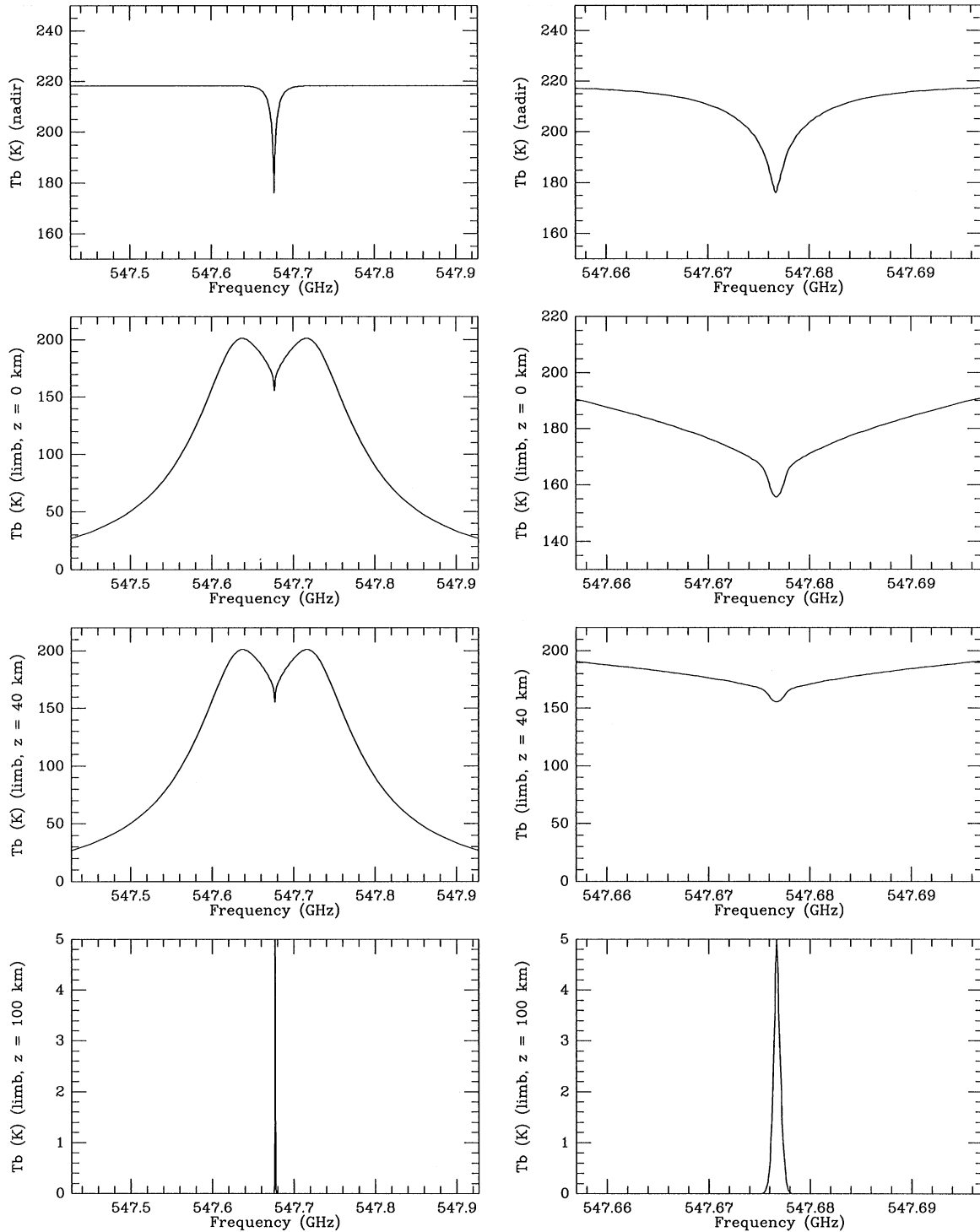


Fig. 8. The H_2^{18}O transition at 556.936 GHz, calculated for nadir, limb and off-limb observations. Left side: 0.5 GHz bandwidth; right side: 40 MHz bandwidth. z is the altitude above the limb, in km.

4.3. MIRO calibration

4.3.1. Radiometric calibration

The absolute calibration of the MIRO instrument will be obtained by observing two loads at different temperatures.

The cold load will be mounted on the spacecraft skin and will be radiatively cooled, while the other will be mounted inside the spacecraft at a nominal temperature of 300 K. The receivers will be calibrated from the measurement of the temperature difference between the two loads. The

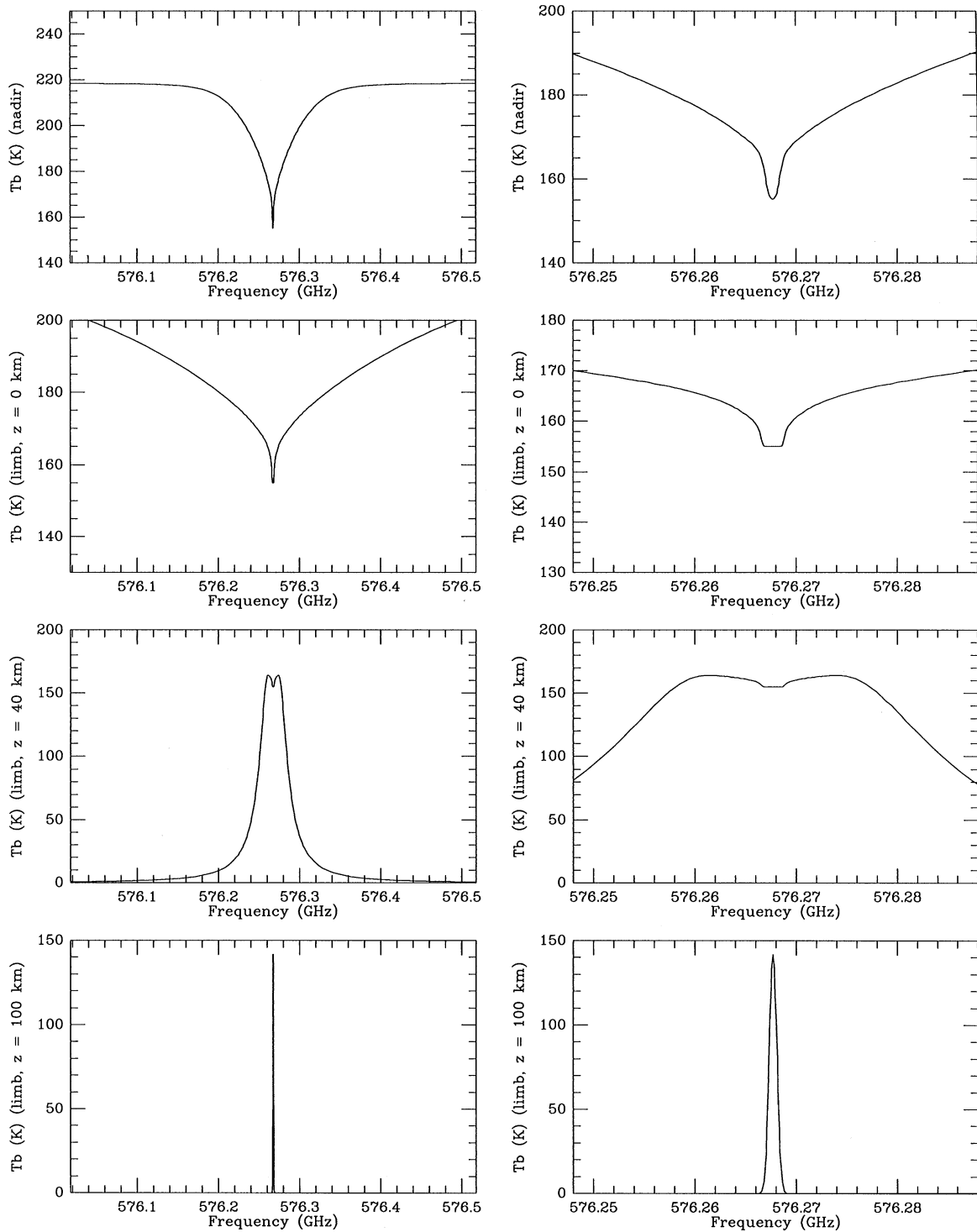


Fig. 9. The CO (5–4) transition at 576.268 GHz, calculated for nadir, limb and off-limb observations. Left side: 0.5 GHz bandwidth; right side: 40 MHz bandwidth. z is the altitude above the limb, in km.

expected accuracy for the absolute spectroscopic calibration is 1 K.

A comparison between the VIRTIS surface temperature and the MIRO subsurface temperatures, at millimeter and submillimeter wavelengths, will provide information upon

the physical properties of the Martian subsurface down to a depth of a few millimeters, possibly up to 1 cm. As mentioned above, the VIRTIS absolute photometric calibration will be checked using the surface temperature data obtained by OMEGA and PFS.

4.3.2. Frequency calibration and wind measurements

For the purpose of frequency calibration, the most favorable position is nadir, because all Doppler shifts related to Mars (either due to the rotation or to atmospheric winds) are equal to zero.

The velocity associated to the planet's rotation is 240 m/s at the equator, which corresponds to a Doppler shift of 446 kHz at 557 GHz. This effect should be observable with MIRO, especially for observations close to the limb. Martian winds in the middle atmosphere can be as high as 150–200 m/s (Lellouch et al., 1991b), and should be also detectable, in spite of the loss of projected spatial resolution (degraded to 20 km) induced by the spacecraft motion.

For both purposes of frequency calibration and wind measurements, the 40 kHz resolution mode would be more favorable. This spectral resolution corresponds to a velocity of about 20 m/s. The corresponding S/N for these observations would thus be degraded by a factor 2.7 as compared to the numbers quoted above. The resulting expected S/N would be in the range 5–7 for surface observations and about 5 for off-limb observations. Thus, in spite of the moderate S/N , it should be possible at least to detect Martian atmospheric winds if their velocity is above 100 m/s.

4.4. Scientific interest of MIRO observations

Muhleman and Clancy (1995) have demonstrated how in-orbit microwave spectroscopy of H₂O and CO could be used for a simultaneous retrieval of the thermal profile and the water vapor distribution, and for a measurement of the Martian winds. Since there is no equivalent to the MIRO instrument on any satellite in-orbit around Mars, the MIRO data should provide the first opportunity for using these techniques. However, as mentioned above, the information to be retrieved from MIRO will be mainly limited by two factors: the small available bandwidth and the high spacecraft velocity. A combination of VIRTIS and MIRO data should allow an improvement of the results. In addition, MIRO data about the surface temperature, the thermal profile and the water content will be coupled with VIRTIS data and compared to OMEGA and PFS results.

5. Conclusions

The Mars flyby of ROSETTA is expected to provide a valuable contribution to the atmospheric and surface science which will be retrieved from Mars Express. It also provides an important opportunity for testing the VIRTIS and MIRO experiments in terms of instrument checking and wavelength/photometric calibration. The observing sequence is expected to last for 15–30 min, depending on the fixed pointing angle, and will require no motion of the platform. The sequence will be performed almost entirely on the dayside, and will include off-limb observations.

The combination of VIRTIS and MIRO datasets will help determining physical parameters like the thermal profile, the H₂O vertical distribution, and the surface and subsurface temperature. In addition, MIRO could possibly provide information on the H₂O vertical distribution at high altitude (from off-limb observations) and on the wind velocity field. From a maximum scientific return of this flyby sequence, coordinated Mars Express and ROSETTA observations should be planned.

Acknowledgements

We wish to thank R.E. Samuelson for helpful comments regarding this paper.

References

- Bibring, J.P., et al., 1991. Topography of the Martian tropical regions with ISM. *Planet. Space Sci.* 39, 225–236.
- Burgdorf, M.J., et al., 2000. ISO observations of Mars: an estimate of the water vapor vertical distribution and the surface emissivity. *Icarus* 145, 79–90.
- Christensen, P.R., et al., 1998. Results from the Mars Global Surveyor Thermal Emission Spectrometer. *Science* 279, 1692–1695.
- Clancy, R.T., Muhleman, D.O., Berge, G.L., 1990. Global changes in the 0–70 km thermal structure of the Martian atmosphere derived from 1975–1989 microwave CO spectra. *J. Geophys. Res.* 95, 14 543–14 554.
- Clancy, R.T., Grossman, A.W., Muhleman, D.O., 1992. Mapping Mars water vapor with the very large array. *Icarus* 100, 48–59.
- Clancy, R.T., et al., 1996. Water vapor saturation at low altitudes around Mars aphelion: a key to Mars climate? *Icarus* 122, 36–62.
- Clark, R.N., Swayze, G.A., Singer, R.B., Pollack, J., 1990. High-resolution reflectance spectra of Mars in the 2.3 μ m region: evidence for the mineral scapolite. *J. Geophys. Res.* 95, 14 463–14 480.
- Coradini, A., et al., 1998. VIRTIS: an imaging spectrometer for the ROSETTA mission. *Planet. Space Sci.* 46, 1291–1304.
- de Graauw, Th., et al., 1997. Observations of Mars with ISO-SWS. *ESA SP-419*, 265–267.
- Drossart, P., et al., 2000. Virtus-H: a high spectral resolution channel for the ROSETTA Infrared Imaging Spectrometer, Spaceborne Remote Sensing VIII, Proceedings of SPIE, Vol 4131, 78–87.
- Encrenaz, T., Lellouch, L., 1990. On the atmospheric origin of weak absorption features in the infrared spectrum of Mars. *J. Geophys. Res.* 95, 14 489–14 494.
- Encrenaz, T., et al., 1991. The atmospheric composition of Mars: ISM and ground-based observational data. *Ann. Geophys.* 9, 797–803.
- Encrenaz, T., et al., 1995. A tentative detection of the 183-GHz water vapor line in the Martian atmosphere: constraints upon the H₂O abundance and vertical distribution. *Icarus* 113, 110–118.
- Erard, S., 1998. A spectrophotometric model of Mars in the near-infrared. *Lunar and Planetary Science XXIX*, abstract #1214. Lunar and Planetary Institute, Houston.
- Erard, S., Calvin, W., 1997. New composite spectra of Mars, 0.4–5.7 μ m. *Icarus* 130, 449–460.
- Gulkis, S., et al., 2001. MIRO: Microwave instrument for the ROSETTA orbiter, *ESA-SP1165*, in press.
- Gurwell, M.A., et al., 2000. SWAS observations of the Martian atmosphere: temperature and vertical distribution of water vapor. *Astrophys. J.* 539, L143–L146.
- Hanel, R.A., et al., 1972. Investigation of the Martian environment by infrared spectroscopy on Mariner 9. *Icarus* 17, 423–442.

- Jacquinet-Husson, N., et al., 1999. The 1997 spectroscopic GEISA databank. *J. Quant. Spectrosc. Radiat. Transfer* 62, 205–254.
- Jakosky, B.M., Haberle, R.M., 1992. The seasonal behavior of water on Mars. In: Kieffer, H.H., et al. (Eds.), *Mars*. University of Arizona Press, Arizona, pp. 969–1016.
- Kakar, R.K., Waters, J.W., Wilson, J.W., 1977. Mars: microwave detection of carbon monoxide. *Science* 196, 1090–1091.
- Kieffer, H.H., Jakosky, B.M., Snyder, C.W., 1992. The planet Mars: from Antiquity to present. In: Kieffer, H.H., et al. (Eds.), *Mars*. University of Arizona Press, Arizona, pp. 1–33.
- Kirkland, L., Forney, P., Herr, K., 1998. Mariner Mars 6/7 infrared spectra: new calibration and a search for water ice clouds, *Lunar and Planetary Science XXIX*, abstract #1516.
- Kurucz, H.L., 1995. The solar spectrum: atlases and line identification. in: Sauval, J., Blomme, R., Grevesse M. (Eds.), *Workshop on laboratory and astronomical high-resolution spectra*. Proceedings of the ASP Conference No. 81, 17 p.
- Lellouch, E., Paubert, G., Encrenaz, T., 1991a. Mapping of CO millimeter-wave lines in Mars'atmosphere: the spatial variability of carbon monoxide on Mars. *Planet. Space Sci.* 39, 219–224.
- Lellouch, E., Goldstein, J.J., Bougher, S.W., Paubert, G., Rosenqvist, R., 1991b. First absolute wind measurements in the middle atmosphere of Mars. *Astrophys. J.* 383, 401–406.
- Lellouch, E., et al., 2000. The 2.4–45 μm spectrum of Mars observed by the Infrared Space Observatory. *Planet. Space Sci.* 48, 1393–1401.
- Muhleman, D.O., Clancy, R.T., 1995. Microwave spectroscopy of the Mars atmosphere. *Appl. Opt.* 34, 6067–6070.
- Pollack, J.P., et al., 1990. Thermal emission spectra of Mars (5.4–10.5 μm): evidence for sulfates, carbonates and hydrates. *J. Geophys. Res.* 95, 14 595–14 627.
- Reininger, F., et al., 1996. VIRTIS: Visible Infrared Thermal Imaging Spectrometer for the ROSETTA mission. *Proc. SPIE* 2819, 66–77.
- Rosenqvist, J., et al., 1992. Minor constituents in the Martian atmosphere from the ISM/Phobos experiment. *Icarus* 98, 254–270.
- Soderblom, L.A., 1992. The composition and mineralogy of the Martian surface from spectroscopic observations. In: Kieffer, H.H., et al. (Eds.), *Mars*. University of Arizona Press, Arizona, pp. 557–593.
- Théodore, B., Lellouch, E., Chassefière, E., Hauchecorne, A., 1993. Solstitial temperature inversions in the Martian middle atmosphere: observational clues and 2-D modeling. *Icarus* 105, 512–528.
- Titov, D.V., et al., 2000. A new method of remote sounding of the martian aerosols by means of spectroscopy in the 2.7 micron CO₂ band. *Planet. Space Sci.* 48, 67–74.
- Zurek, R.W., Barnes, J.R., Haberle, R.M., Pollack, J.B., Tillman, J.E., Leovy, C.B., 1992. Dynamics of the atmosphere of Mars. In: Kieffer, H.H., et al. (Eds.), *Mars*. University of Arizona Press, Arizona, pp. 835–933.